iJRASET
International Journal For Research in Applied Science and Engineering Technology

INTERNATIONAL JOURNAL FOR RESEARCH

IN APPLIED SCIENCE & ENGINEERING TECHNOLOGY

Volume: 9 **Issue:** X **Month of publication:** October 2021

DOI: https://doi.org/10.22214/ijraset.2021.38538

www.ijraset.com

Call: 08813907089 | E-mail ID: ijraset@gmail.com

International Journal for Research in Applied Science & Engineering Technology (IJRASET)
ISSN: 2321-9653; IC Value: 45.98; SJ Impact Factor: 7.429
Volume 9 Issue X Oct 2021- Available at www.ijraset.com

Study for Improvement in the Surface Properties and Wear Behavior of Mild Steel

Hamdan Gowhar Nahvi[1], Gurlal Singh[2]
[1, 2]*Department of Mechanical Engineering, Desh Bhagat University, Mandi Gobindgarh*

Abstract: ***Surface of a material can be improved by depositing the filler metal for the enhancement of various properties. Surface should be harder than substrate material for surface improvement. This surface improvement is also known as surfacing. In present research Mild steel specimens of size 140×35×40 were used to deposit surfacing layers and study the feasibility of iron/aluminum with varying compositions on low carbon steel deposited by GTAW process. Specimens for hardness and oxidation resistance were prepared. While studying oxidation of surfaced and un-coated area (base material), oxidation test resulted that the oxidation occurred on surface of base metal (un-coated area) after heating at different temperatures and time intervals. Specimens kept at 500˚C, 700˚C temperatures for 3, 6, 9 hours to get oxidized from un-coated surface but no mark of oxidation and pitting was visible at surfaced area but pitting of un-coated area occurred at 700˚C temperature. Oxidation had no effect to surfaced area. Low temperature oxidation test specimens gave only weight loss from un-coated portion but high temperature oxidation gave high amount of weight reduction due to pitting occurred on un-coated portion. The amount of weight loss of specimens increased with increase in furnace holding time at constant temperature. With increase in temperature oxidation of un-coated area of specimens also increased and pitting action occurred on un-coated area of specimens at high temperature. Further, for the various wear tests the cylindrical pins of 8 mm diameter with spherical tip 4 mm radius was made. Wear tests were carried out on pin on disc sliding wear testing machine. The comparison of wear rate loss was studied with constant sliding distance, varying load and sliding velocity of different compositions of iron/aluminum surfacing and substrate material. Hardness and wear resistance of composition were increased with increase in percentage of Fe element in composition. Composition C1 (Fe:Al/70:30) had high hardness and high wear resistance as compared to composition C2 (Fe:Al/30:70) and C3 (Fe:Al/50:50). Composition C3 (Fe:Al/50:50) had better hardness and wear resistance as compared composition C2 (Fe:Al/70:30).***

Keywords: Surface improvement, Fe-Al intermetallic, GTAW process, Sliding wear.

I. INTRODUCTION

Welding is a fabrication process used to join two materials (metals or thermoplastics) permanently, by melting of work pieces at the joining interface through localized coalescence resulting from a suitable combination of temperature, pressure with metallurgical conditions, with the use of filler material added to molten material pool (weld pool) or not. After solidification of molten metal pool, it becomes strong joint.

The gas tungsten arc welding (GTAW) process is based on the electric arc established between a non-consumable electrode of tungsten and the work-pieces to be joined. Part of the heat generated by the electric arc is added to the workpieces, promoting the formation of a weld pool.

The weld pool is protected from air contamination by a stream of an inert gas (Ar or He) or a mixture of gases. GTAW can use a positive direct current, negative direct current or an alternating current, depending on the power supply set up. A negative direct current from the electrode causes a stream of electrons to collide with the surface, generating large amounts of heat at the weld region.

This creates a deep, narrow weld. In the opposite process where the electrode is connected to the positive power supply terminal, positively charged ions flow from the tip of the electrode instead, so the heating action of the electrons is mostly on the electrode. This mode also helps to remove oxide layers from the surface of the region to be welded, which is good for metals such as Aluminum or Magnesium.

A shallow, wide weld is produced from this mode, with minimum heat input. Alternating current gives a combination of negative and positive modes, giving a cleaning effect and imparts a lot of heat as well. The autogeneous process is readily used in robotics, although special techniques are needed when it is necessary to add filler metal to the weld pool.

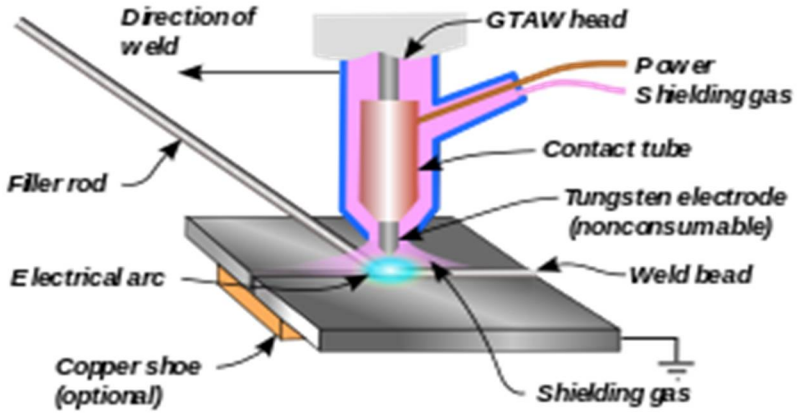

Fig 1. GTAW process set up

II. LITERATURE SURVEY

1) **Kumar et al. (1)** shows the effect of arc oscillations in improving the mechanical properties of Steel/Aluminium lap joints in the GTAW process. Arc oscillations produce the weaving pattern to manipulate the heat energy density on the base metal. Fe-Al joints were prepared with different heat inputs by varying the welding current and welding speed. The thermal profile and the intermetallic compound layer results indicate the decrease in heat energy density with arc oscillations. Further, the mechanical properties of the joints were compared with no weaving condition and found the enhancement in aesthetics, microhardness, and failure strength of the Fe-Al joints with arc oscillations. **Kumar et al.** used GTAW to join AA5061-T6 and galvannealed (GA) steel. The welding current distributed in sine, rectangle, square, and triangle AC waveform is used to understand their influence on the arc behavior, temperature distribution, joint profile, and the intermetallic compound (IMC) layer thickness. The instantaneous welding current and voltage waveforms are recorded in synchronization with the high-speed arc images to understand the arc behavior and heat input. The rate of change of instantaneous welding current between the polarities and the arc duration at the peak current is more in square and rectangle waveforms. The peak current in both the positive and negative pulses and the arc heat input of the triangle waveform is the highest among all the waveforms considered in the present work. The wetting length increases along with the reduction in the bead height sequentially with sine, rectangle, square, and triangle waveforms for a constant machine setting welding current. IMC layer thickness is minimum for the sine waveform and maximum for the triangle waveform. Overall, the welding current distributed in sine waveform is found to be suitable among all the waveforms studied in the present work for dissimilar metal joining of aluminum to steel.
2) **Subramani et al. (2)** fabricated a composite through the TIG (Tungsten inert gas) welding setup. In this new era, the composite materials play a vital role in all applications. Hybrid composites are composites that comprise two or more fibres or matrixes in their lamina. Alloys of aluminium are unanimously used in aircraft, aerospace and transportation industries due to their high strength to weight ratio. In this project, the particle reinforced metal matrix composites (PRMMC) were produced by using TWP (TIG Welding Process). The PRMMC manufactured through this process are Sic/B4C/A5061, Sic/graphite/A5061 and A5061/graphite/B4C/Sic. The SEM (scanning electron microscopy), XRD tests were conducted to illustrate the status and properties of samples. Uniform distribution of reinforcements in the hybrid composites is a direct sign of enriching the mechanical properties of three Al5061 plates. Pretending the mechanical behaviour of hybrid composites is always significant to find the safety of the composites.
3) **Ebrahimzadeh et al. (3)** studied the microstructure and the mechanical behavior of the butt weld joints of the aluminum 0.9 mm thin sheet of Al 5456 Al alloys produced by GTAW and GMAW process were studied using two pulse and alternative currents. The results showed that microstructure of the weld metal of all GTAW samples contained a dendritic structure; this was such that the finer grain sizes were obtained in the weld metal of the pulsed samples, whereas by increasing the pulsed time, the grain growth was observed in the GTAW process. In the tension tests, all weldments failed from the HAZ zone, but the two samples welded by GTAW process with 0.2 and 0.3 pulsed time were failed from the base metal. Maximum and minimum tensile strength was obtained in the samples welded by GTAW process with 0.2 pulsed time and the MIG process samples, which was about 5.93% and 32.95 compare to base metal, respectively.

4) **Gill et al. (4)** investigated the deposition of iron-aluminium intermetallic over a low carbon substrate using gas tungsten arc welding (GTAW) process. Oxidation resistance of the iron and aluminium metal powders deposits in varying ratios and few mechanical and metallurgical properties such as microhardness, microstructure and wear resistance.
5) **Borrisutthekul et al. (5)** study the effect of zinc-coated layer on steel sheet of dissimilar metals welding between SCGA270C steel and A5052 aluminum alloy by GTAW was investigated. In the experiments, two types of self-brazing welding; 1) welding between non-zinc-coated steel/aluminum alloy, and 2) welding between zinc-coated steel/aluminum alloy, were carried out. The lap joint configuration in which steel was lying on top of aluminum alloy was applied. From the results of zinc-coated steel case, the reaction between the low melting-point zinc with both molten and solid aluminum alloy provided larger welding width between two metal sheets. Moreover, zinc, which is heavier than aluminum alloy, was fallen down but not well mixed into molten aluminum alloy. Consequently, thick intermetallic compound layer near welding interface between steel/aluminum alloy was formed. However, when applying higher, significant contraction of aluminum welding pool promoted crack along the non-uniform chemical composition zone in case of zinc-coated steel. These cracks were the cause of reduction of load resistance of the welds between zinc-coated steel/aluminum alloy.
6) **Huang et al. (6)** study the effect of welding conditions on the formation of porosity. Two conditions involved in the preparation of base metals were discussed: the application of a groove and thickness of the welding root face. Spectral analyses based on data mining and empirical mode decomposition (EMD) were proposed to detect porosity. Spectral lines were identified accurately by data mining based on an improved K-medoids algorithm which ascertained the classification number using a geodesic minimum spanning tree. EMD was employed to eliminate effectively the influence of noise and a pulsed current on spectral intensity ratio, resulting in clear characteristic values used for detection of pores. X-ray analyses verified the proposed method and showed that the welding conditions significantly affected the size and distribution of pores. The results indicated that the weld quality was improved with the application of a groove. And the number of pores and pores area decreased significantly when the thickness of the welding root face was 2 mm.
7) **Almenara et al. (7)** investigates the influence of welding parameters on the microstructure and mechanical properties of GTAW welded AA6105 aluminum alloy joints. AA6105 alloy plates with different percent values of cold work were joined by GTAW, using various combinations of welding current and speed. The fusion zone, in which the effects of cold work have disappeared, and the heat affected zone of the welded samples were examined under optical and scanning electron microscopes; additionally, mechanical tests and measures of Vickers micro hardness were performed. Results showed dendritic morphology with solute micro- and macrosegregation in the fusion zone, which is favored by the constitutional super cooling when heat input increases. When heat input increased and welding speed increased or remained constant, greater segregation was obtained; whereas welding speed decrease produced a coarser microstructure. In the heat affected zone recrystallization, dissolution, and coarsening of precipitates occurred, which led to variations in hardness and strength.

III. OBJECTIVES OF PRESENT INVESTIGATION:

A. To study the feasibility of new technique using a layer of Fe-Al compound on the surface of work piece with TIG welding process.
B. Comparative Study of micro-hardness and wear behaviour by varying percentage of Fe-Al powder to coated material.

IV. EXPERIMENTATION

The present work was carried out to study experimentally the effect of Fe-Al surfacing on low carbon steel by varying compositions with aim to enhancement in surface properties and wear behavior.

A. Selection of Base Metal

Mild steel was selected as base material for surfacing purpose, as knew that it is mainly used in wide application in the fabrication industry. The general composition of mild steel is given in table 1.

Table 1 showing composition of mild steel

Element	C	Mn	Cr	Mo	Ni	Si	S	Al	Cu	Fe
percentage	0.114	0.6	0.034	0.013	0.018	0.043	0.015	0.019	0.042	remaining

B. Selection of Metal Powder

There are no sources in the current document.

Fe and Al metal powders were selected for surfacing of mild steel. Different compositions of both powders were prepared by weight and applied by mixing with acetone to form paste.

Fe: - Metal powder of 350 mesh size

Al: - Fine metal powder

C. Compositions of Powders Used

Table 2 shows compositions of powders by varying percentages.

Metal powder	Al %	Fe %
Composition 1 (C1)	30	70
Composition 2 (C2)	70	30
Composition 3 (C3)	50	50

D. Preparation of Base Material

Three mild steel specimens (140×35×40) mm had been selected. The specimens were cut into required length with the help of a power hacksaw. The specimens were machined on shaper machine for rectangular shape groove of size 12×4 mm to guide the powder paste. The mild steel specimens were taken as the base metal or substrate material upon which the surfacing material was deposited by GTA welding after the application of paste. Before depositing the surfacing material the specimens were thoroughly prepared by mechanically and chemically cleaned in order to avoid experimental errors.

E. Preparation of Fe-Al Powder Mixture

The mixture of iron and aluminum powders with percentages 70:30, 50:50, 30:70 were used as surfacing material. For surfacing this steel, there was no need of pre-heating operation. Acetone was used to locate the powder mixture in the guided groove of substrate surface.

F. Parameters Used for Pin on Disc Wear Test Machine

Table 3 parameters for sliding wear testing.

Compositions	Load (N)	Time (sec)	Sliding speed (rpm)	Track diameter (mm)	Distance covered (mm)
C1	30	300	300	50	186200
C2	50	150	500	50	186200
C3	70	100	700	70	186200

V. RESULT AND ANALYSIS

The oxidation resistance of the surfaced area was evaluated by heating to the temperatures of 500 and 700˚C and holding for 3, 6, and 9 hours. After heating in furnace specimens had been cooled in air for 12 hours. Samples were washed with acetone before and after performing experiment for weighing. Qualitative analysis of oxidation test had been taken by change in total weight loss after heating in furnace and holding at different temperatures and time intervals respectively.

Table 4: Data of Oxidation Test Results

Sr no.	Temperature (˚C)	Time (hrs)	Initial wt. (g)	Final wt. (g)	Total wt. loss (g)
1	500˚C	3	51.4628	51.4531	0.0097
2		6	44.1504	44.1491	0.0113
3		9	53.0782	53.0593	0.0189
4	700˚C	3	41.2015	41.1016	0.0999
5		6	55.5028	55.4547	0.1481
6		9	21.0371	20.8134	0.2237

Table 4 gives oxidation of specimen no. 4 has been placed in furnace for 3 hours at 700˚C temperature which gives minimum weight loss of 0.0999 g from un-coated region with 95.04 % of total area of specimen. Specimen no. 2 gives weight loss of 0.1481g after heating in furnace for 6 hours at 700˚C temperature from un-coated region with 93.63 % of total area of specimen. Specimen no. 3 gives maximum weight loss of 0.2237 g at 700˚C temperature for 9 hours from un-coated region with 88.7 % of total area of specimen.

Hardness is ability of metal to resist penetration and abrasion wear. The measurements of hardness provide information of metallurgical changes caused by welding. The Vickers hardness tester was used for all prepared specimens to take the measurements of weld area under the constant load of 500 gm. The hardness values have been taken along the x-x axis with difference of 1 mm distance and y-y axis with difference of 0.5 mm distance. Then, average value of each composition has been calculated.

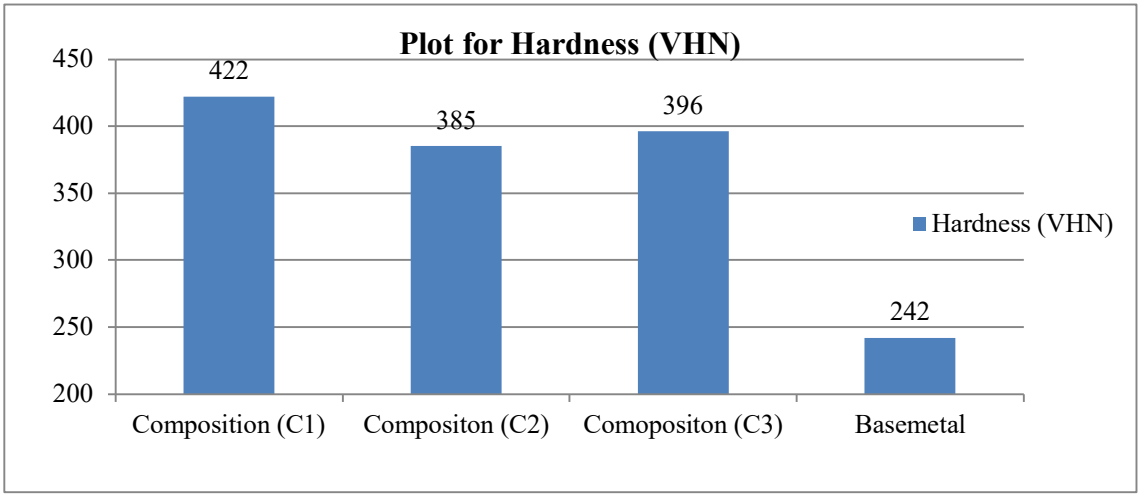

Fig. 2: Comparison of Micro Hardness measurement

Wear is damage to a surface of body as a result of relative motion with respect to another surface under load in dry conditions. This test had been performed in three sets. Each set has different parameters by varying load, track diameter, time, sliding speed (rpm) but constant sliding distance. Wear tests were performed under normal atmospheric conditions. All the specimens prior and after the test were cleaned with acetone and weighed with digital electronic balance having accuracy of ±0.001 g. Difference between initial weight and final weight gave the total weight loss after sliding wear test. Wear rate is considered by total weight loss during experiment. Table shows the results performed in sets.

Calculation formula for wear rate (mg/hr) = $\frac{(\text{Final wt.} - \text{Initial wt.})}{\text{Time (minute)}} \times 50 \times 1000$

Composition (C_1) (Fe:Al / 70:30)								
	Initial wt. (g)	Final wt. (g)	Weight loss (g)	Time (sec)	Wear rate (mg/hr)	Load (N)	Sliding speed (rpm)	Hardness (VHN)
1	15.1944	15.1930	0.0004	300	3.4	30	300	422
2	13.5621	13.5614	0.0007	300	7	50	300	422
3	12.9664	12.9655	0.0009	300	9.4	70	300	422
4	13.6722	13.6716	0.0006	150	11	30	500	422
5	12.8459	12.8451	0.0008	150	21	50	500	422
6	12.4989	12.4979	0.0010	150	28.5	70	500	422
7	12.5837	12.5830	0.0007	100	26.70	30	700	422
8	12.7826	12.7816	0.0010	100	30.55	50	700	422
9	12.3769	12.3757	0.0012	100	58.70	70	700	422

Table 5: Data of wear test of composition (C_1) (Fe:Al / 70:30)

1) *Discussion of Wear Test of Composition (C_1) (Fe:Al /70:30):* Results in Table 5 give the data of wear test. The data gives the value at different loads, different sliding speeds (rpm) and constant sliding distance (m).

A. Effect of Sliding Speeds (RPM) on Wear Rate with Varying Loads (N)

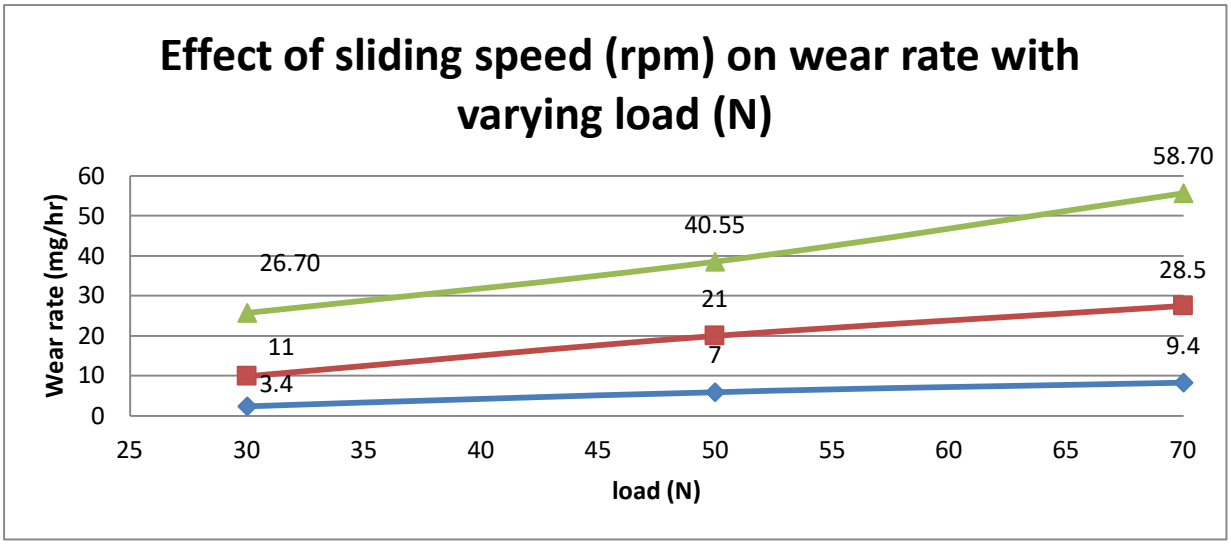

Fig 3: Effect of sliding speed (rpm) on wear rate with respect to varying load (N)

Fig. 3 shows the effect of wear rate (mg/hr) of composition (C_1) (Fe:Al/70:30) at different constant sliding speeds 300, 500, 700 rpm respectively at constant sliding distance 186.2 m with varying loads 30, 50 and 70 N each. Fig. 3 reveals that as the load is increasing at constant sliding speeds, wear rate is also increasing. Fig. 3 shows values of wear rate at constant sliding speed 300 rpm, are observed as 3.4 mg/hr at load 30N, 7 mg/hr at load 50N, and 9.4mg/hr at load 70 N. Wear rate at constant sliding speed 500 rpm is observed as 11 mg/hr at load 30N, 21 mg/hr at load 50N, and 28.5 mg/hr at load 70 N. Wear rate at constant sliding speed 700 rpm is also observed as 26.70 mg/hr at load 30N, 30.55 mg/hr at load 50N, and 58.70 mg/hr at load 70 N. The wear rate is minimum at lower load and maximum at higher load with constant sliding speed. Due to increase in load at constant sliding speed, pressure at interface between pin and disc also increasing, this causes the wear of pins. Fig. 3 also gives different slopes of trend lines at different sliding speeds. The slope of trend line at constant sliding speed 300 rpm shows negligible effect of varying loads to composition C_1, whereas trend line at constant sliding speed 500 rpm shows slightly high effect of loads as compared to sliding speed 300 rpm. Slope of trend line at constant sliding speed 700 rpm shows heavily effect of loads as compared to both sliding speeds 300 and 500 rpm respectively**.**

B. Effect of loads (N) on wear rate with varying sliding speeds (rpm)

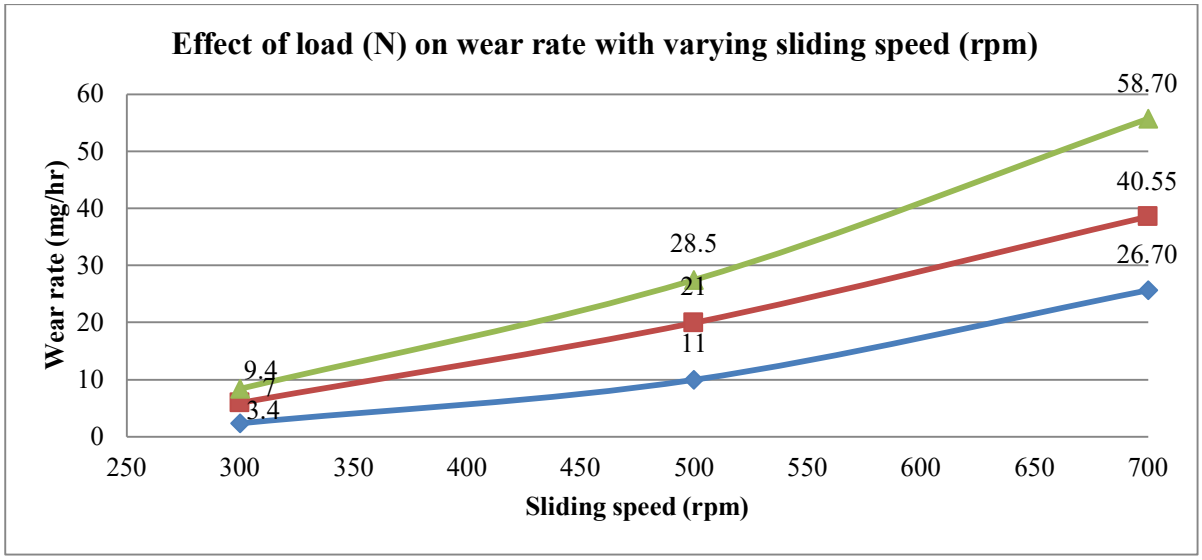

Fig 4: Effect of loads (N) on wear rate with varying sliding speeds (rpm)

Fig. 4 shows the effect of wear rate (mg/hr) of composition (C_1) (Fe:Al/70:30) at different constant loads 30, 50, 70N and constant sliding distance 186.2 m with varying sliding speeds 300, 500 and 700 rpm. Fig. 4.5 reveals that as the sliding speed is increasing at constant load, wear rate is also increasing. Fig. 4.5 shows values of wear rate at constant load 30 N, are observed as 2.4 mg/hr at sliding speed 300 rpm, 10 mg/hr at sliding speed 500 rpm, and 25.71 mg/hr at sliding speed 700 rpm. Wear rate at constant load 50 N is observed as 6 mg/hr at sliding speed 300 rpm, 20 mg/hr at sliding speed 500 rpm, and 38.57 mg/hr at sliding speed 700 rpm. Wear rate at constant load 70 N is also observed as 8.4 mg/hr at sliding speed 300 rpm, 27.5 mg/hr at sliding speed 500 rpm, and 55.71 mg/hr at sliding speed 700 rpm. The wear rate was minimum at lower load and maximum at higher load. The reason behind this is, with increase in sliding speed at constant load, time taken by a particular point for making one rotation decrease and heat generation at interface between pin and disc also increasing. High sliding speed at constant load gives short time period for one rotation and high heat generation. With increase in heat generation to surfaced material and less time is taken to cool down the interface so it lost its hardness properties and decrease in wear resistance, which caused the wear of pins. This shows the low wear rate at minimum sliding speed and high wear rate at maximum sliding speed at constant load. Fig. 4 also gives different slopes of trend lines at different loads. The slope of trend line at constant load 30 N shows lesser effect of varying sliding speeds to composition C_1 than slope of trend line of 50 and 70 N respectively, whereas trend line at constant load 50 N shows slightly high effect of sliding speeds as compared to load 30 N. Slope of trend line at constant load 70 N shows heavily effect of sliding speeds as compared to both loads 30 and 50 N respectively.

1) *Discussion of Wear Test of Composition (C_2) (Fe:Al / 30:70):* Results in Table 6 give the data of wear test. The data gives the value at different loads, different sliding speeds (rpm) and constant sliding distance.

Table 6: Data of Wear Test composition (C_2) (Fe:Al / 30:70)

Composition (C_2) (Fe:Al/ 30:70)									
	Initial wt. (g)	Final wt. (g)	Weight loss (g)	Time (sec)	Track dia.(mm)	Wear rate (mg/hr)	Load (N)	Sliding speed (rpm)	Hardness (VHN)
1	12.8146	12.8139	0.0007	300	30	10.6	30	300	385
2	12.7481	12.7471	0.0010	300	30	14.2	50	300	385
3	12.9941	12.9928	0.0013	300	30	17.8	70	300	385
4	12.8384	12.8374	0.0010	150	50	23.5	30	500	385
5	13.5166	13.5154	0.0012	150	50	33.5	50	500	385
6	13.3539	13.3525	0.0014	150	50	40	70	500	385
7	12.7712	12.7700	0.0012	100	50	48.14	30	700	385
8	12.6960	12.6949	0.0011	100	50	51	50	700	385
9	12.5775	12.5757	0.0020	100	50	82.43	70	700	385

C. Effect of sliding speeds (rpm) on wear rate with varying loads (N)

Fig. 5 shows the effect of wear rate (mg/hr) of composition (C_2) (Fe:Al/30:70) at different constant sliding speeds 300, 500, 700 rpm respectively at constant sliding distance 186.2 m with varying loads 30, 50 and 70 N each. Fig. 5 reveals that as the load is increasing at constant sliding speeds, wear rate is also increasing.

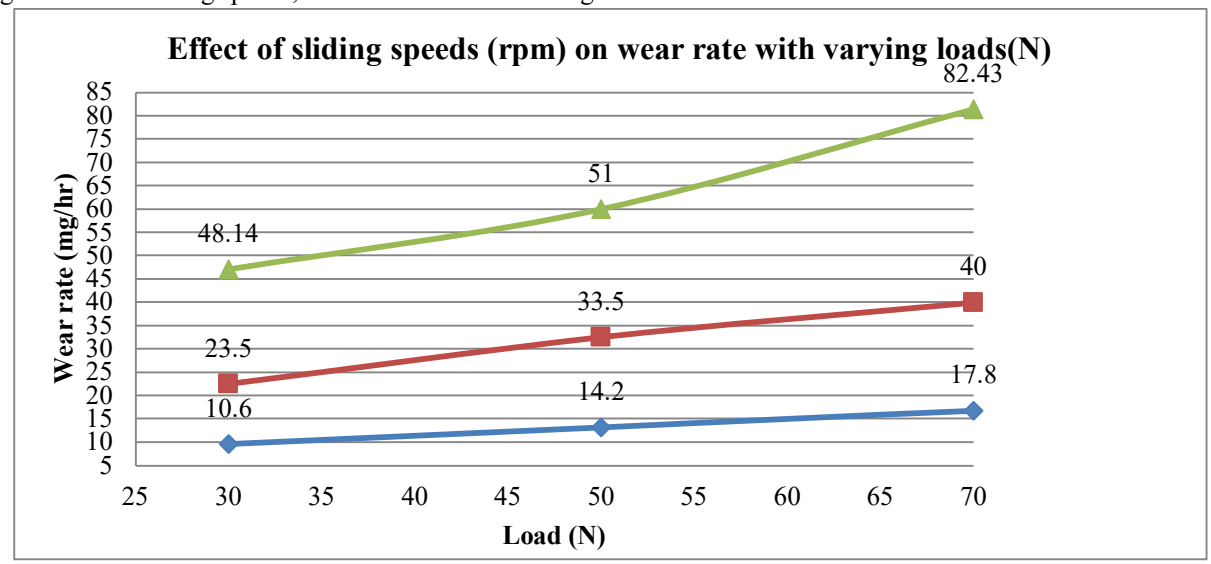

Fig 5: Effect of sliding speeds (rpm) on wear rate with varying loads (N)

Fig. 5 shows values of wear rate at constant sliding speed 300 rpm, are observed as 10.6 mg/hr at load 30N, 14.2 mg/hr at load 50N, and 17.8 mg/hr at load 70 N. Wear rate at constant sliding speed 500 rpm is observed as 23.5 mg/hr at load 30N, 33.5 mg/hr at load 50N, and 30 mg/hr at load 70 N. Wear rate at constant sliding speed 700 rpm is also observed as 48.14 mg/hr at load 30N, 51 mg/hr at load 50N, and 82.43 mg/hr at load 70 N. The wear rate is minimum at lower load and maximum at higher load with constant sliding speed. Due to increase in load at constant sliding speed, pressure at interface between pin and disc also increasing, this causes the wear of pins. Fig. 5 also gives different slopes of trend lines at different sliding speeds. The slope of trend line at constant sliding speed 300 rpm shows negligible effect of varying loads to composition C_2, whereas trend line at constant sliding speed 500 rpm shows slightly high effect of loads as compared to sliding speed 300 rpm. Slope of trend line at constant sliding speed 700 rpm shows heavily effect of loads as compared to both sliding speeds 300 and 500 rpm respectively.

D. Effect of loads (N) on wear rate (mg/hr) with varying sliding speeds (rpm)

Fig. 6 shows the effect of wear rate (mg/hr) of composition (C_2) (Fe:Al/30:70) at different constant loads 30, 50, 70N and constant sliding distance 186.2 m with varying sliding speeds 300, 500 and 700 rpm. Fig. 6 reveals that as the sliding speed is increasing at constant load, wear rate is also increasing.

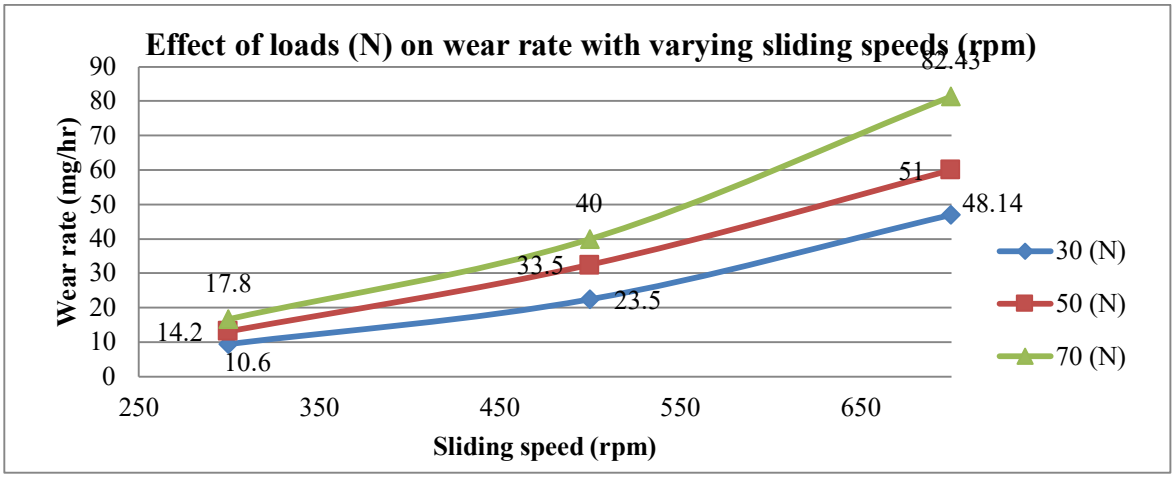

Fig 6: Effect of loads (N) on wear rate (mg/hr) with varying sliding speeds (rpm)

Fig. 6 shows values of wear rate at constant load 30 N, are observed as 10.6 mg/hr at sliding speed 300 rpm, 23.5 mg/hr at sliding speed 500 rpm, and 48.14 mg/hr at sliding speed 700 rpm. Wear rate at constant load 50 N is observed as 14.2 mg/hr at sliding speed 300 rpm, 33.5 mg/hr at sliding speed 500 rpm, and 51 mg/hr at sliding speed 700 rpm. Wear rate at constant load 70 N is also observed as 17.8 mg/hr at sliding speed 300 rpm, 40 mg/hr at sliding speed 500 rpm, and 82.43 mg/hr at sliding speed 700 rpm. The wear rate was minimum at lower load and maximum at higher load. The reason behind this is, with increase in sliding speed at constant load, time taken by a particular point for making one rotation decrease and heat generation at interface between pin and disc also increasing. High sliding speed at constant load gives short time period for one rotation and high heat generation. With increase in heat generation to surfaced material and less time is taken to cool down the interface so it lost its hardness properties and decrease in wear resistance, which caused the wear of pins. This showed the low wear rate at minimum sliding speed and high wear rate at maximum sliding speed at constant load. Fig. 6 also gives different slopes of trend lines at different loads. The slope of trend line at constant load 30 N shows lesser effect of varying sliding speeds to composition C_2 than slope of trend line of 50 and 70 N respectively, whereas trend line at constant load 50 N shows slightly high effect of sliding speeds as compared to load 30 N. Slope of trend line at constant load 70 N shows heavily effect of sliding speeds as compared to both loads 30 and 50 N respectively.

1) *Discussion of wear test of composition (C_3) (Fe:Al / 50:50):* Results in Table 7 give the data of wear test. The data gives the value at different loads, different sliding speeds (rpm) and constant sliding distance.

Table 7: Data of sliding wear test results of composition C_3

Composition C3 (Fe:Al/50:50)								
	Initial wt. (g)	Final wt. (g)	Weight loss (g)	Time (sec)	Wear rate (mg/hr)	Load (N)	Sliding speed (rpm)	Hardness (VHN)
1	12.5171	12.5166	0.0005	300	5.8	30	300	396
2	12.5292	12.5283	0.0009	300	11.8	50	300	396
3	12.7334	12.7322	0.0012	300	15.4	70	300	396
4	12.8239	12.8232	0.0007	150	16	30	500	396
5	12.7875	12.7864	0.0011	150	28.5	50	500	396
6	13.0872	13.0856	0.0016	150	38.5	70	500	396
7	12.8419	12.8411	0.0008	100	35.29	30	700	396
8	12.3521	12.3509	0.0012	100	52.43	50	700	396
9	12.8994	12.8978	0.0016	100	69.57	70	700	396

E. Effect of sliding speeds (rpm) on wear rate with respect to varying loads (N)

Fig. 7 shows the effect of wear rate (mg/hr) of composition (C_3) (Fe:Al/50:50) at different constant sliding speeds 300, 500, 700 rpm respectively at constant sliding distance 186.2 m with varying loads 30, 50 and 70 N each. Fig. 7 reveals that as the load is increasing at constant sliding speeds, wear rate is also increasing. Fig. 7 shows values of wear rate at constant sliding speed 300 rpm, are observed as 5.8 mg/hr at load 30N, 11.8 mg/hr at load 50N, and 15.4 mg/hr at load 70 N. Wear rate at constant sliding speed 500 rpm is observed as 16 mg/hr at load 30N, 28.5 mg/hr at load 50N, and 38.5 mg/hr at load 70 N. Wear rate at constant sliding speed 700 rpm is also observed as 35.29 mg/hr at load 30N, 52.43 mg/hr at load 50N, and 69.57 mg/hr at load 70 N.

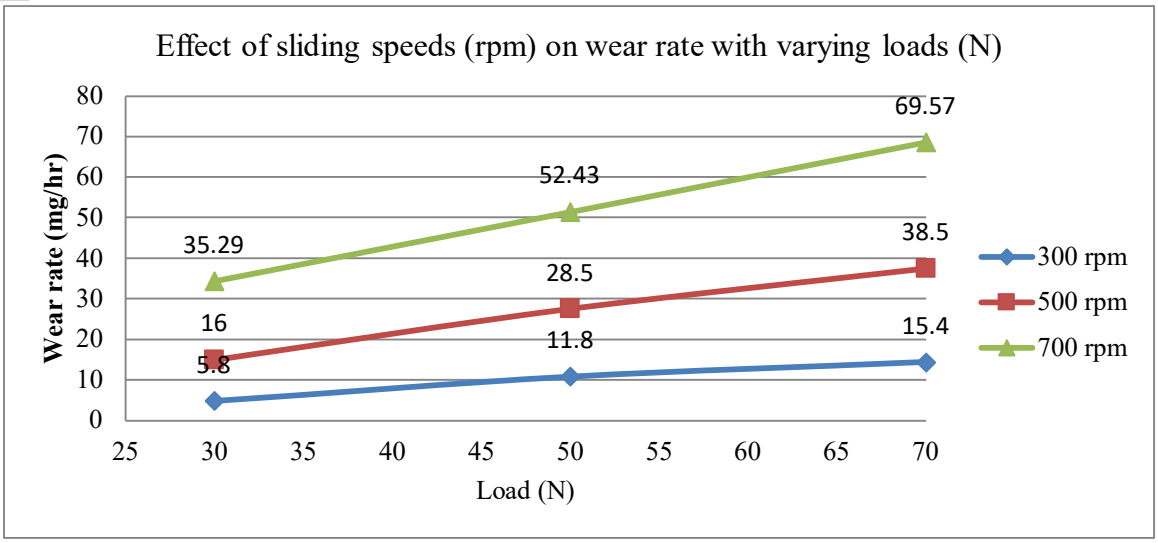

Fig 7: Effect of sliding speeds (rpm) on wear rate with respect to varying loads (N)

The wear rate is minimum at lower load and maximum at higher load with constant sliding speed. Due to increase in load at constant sliding speed, pressure at interface between pin and disc also increasing, this causes the wear of pins. Fig. 7 also gives different slopes of trend lines at different sliding speeds. The slope of trend line at constant sliding speed 300 rpm shows negligible effect of varying loads to composition C_3, whereas trend line at constant sliding speed 500 rpm shows slightly high effect of loads as compared to sliding speed 300 rpm. Slope of trend line at constant sliding speed 700 rpm shows heavily effect of loads as compared to both sliding speeds 300 and 500 rpm respectively**.**

F. Effect of loads (N) on wear rate with respect to varying sliding speed (rpm)

Fig. 8 shows the effect of wear rate (mg/hr) of composition (C_3) (Fe:Al/50:50) at different constant loads 30, 50, 70N and constant sliding distance 186.2 m with varying sliding speeds 300, 500 and 700 rpm. Fig. 8 reveals that as the sliding speed is increasing at constant load, wear rate is also increasing. Fig. 8 shows values of wear rate at constant load 30 N, are observed as 5.8 mg/hr at sliding speed 300 rpm, 16 mg/hr at sliding speed 500 rpm, and 35.29 mg/hr at sliding speed 700 rpm. Wear rate at constant load 50 N is observed as 11.8 mg/hr at sliding speed 300 rpm, 28.5 mg/hr at sliding speed 500 rpm, and 52.43 mg/hr at sliding speed 700 rpm. Wear rate at constant load 70 N is also observed as 15.4 mg/hr at sliding speed 300 rpm, 38.5 mg/hr at sliding speed 500 rpm, and 69.57 mg/hr at sliding speed 700 rpm.

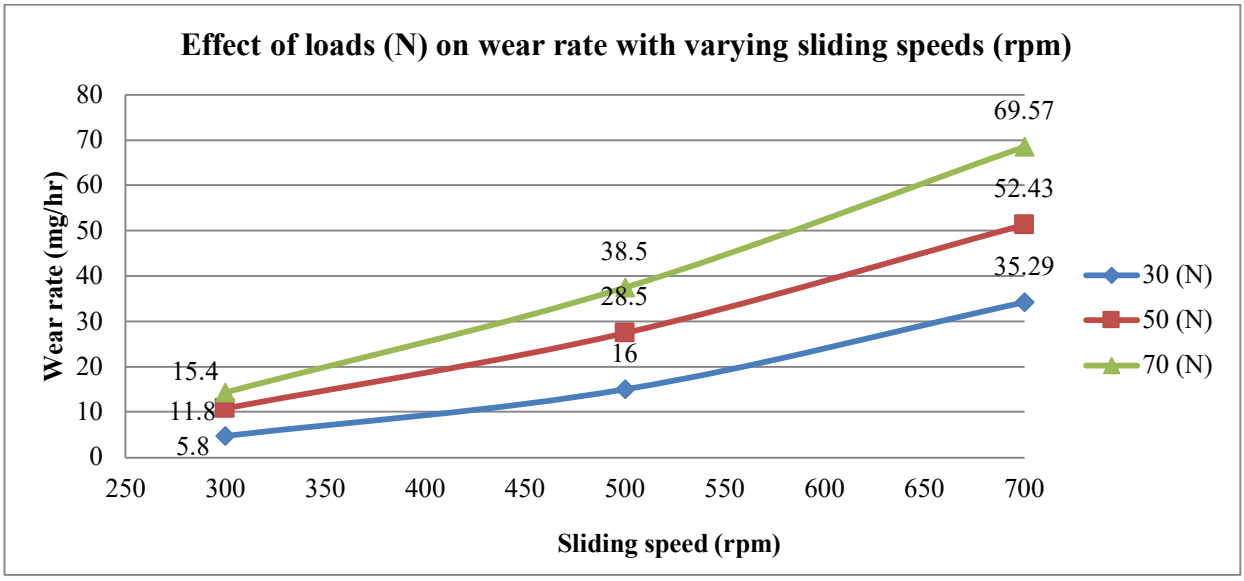

Fig 8: Effect of loads (N) on wear rate with respect to varying sliding speed (rpm)

The wear rate was minimum at lower load and maximum at higher load. The reason behind this is, with increase in sliding speed at constant load, time taken by a particular point for making one rotation decrease and heat generation at interface between pin and disc also increasing. High sliding speed at constant load gives short time period for one rotation and high heat generation. With increase in heat generation to surfaced material and less time is taken to cool down the interface so it lost its hardness properties and decrease in wear resistance, which caused the wear of pins. This showed the low wear rate at minimum sliding speed and high wear rate at maximum sliding speed at constant load. Fig. 8 also gives different slopes of trend lines at different loads. The slope of trend line at constant load 30 N shows lesser effect of varying sliding speeds to composition C_3 than slope of trend line of 50 and 70 N respectively, whereas trend line at constant load 50 N shows slightly high effect of sliding speeds as compared to load 30 N. Slope of trend line at constant load 70 N shows heavily effect of sliding speeds as compared to both loads 30 and 50 N respectively.

VI. CONCLUSION

A. From the results of oxidation experiments, the weight loss for 500ºC temperature with increase of time interval is 3 hrs < 6 hrs < 9 hrs and no pitting action. The weight loss for 700ºC temperature with increase of time interval is 3 hrs < 6 hrs < 9 hrs and pitting action occurs on all specimens. The weight loss of specimens is increasing in amount with increase in holding time in furnace at constant temperature.

B. Experiments also give conclusion of weight loss at 500ºC temperature for 3 hrs with no pitting < 700ºC temperature for 3 hrs with pitting action, Weight loss at 500ºC temperature for 4 hrs with no pitting < 700ºC temperature for 6 hrs with pitting action, weight loss at 500ºC temperature for 8 hrs with no pitting < 700ºC temperature for 8 hrs with pitting action. The weight loss is also increasing with the increase in temperature for a particular interval of time.

C. From the results of hardness tests, hardness is increasing with increase in percentage of Fe element to the filler material. It can be easily concluded that composition C_1 of surfaced material has better results than composition C_2, C_3 and base metal. So the hardness trend is composition C_1 (Fe:Al / 70:30) > C_2 (Fe:Al / 30:70) > C_3 (Fe:Al / 50:50) > base metal.

REFERENCES

[1] Kumar, T., Kiran, D.V., Arora, N. and Chitral, S. (2021), "Manipulating heat density to enhance the performance of Aluminium Alloy-Steel joints using arc oscillations in the GTAW process", Materials Letters, Vol. 306.
[2] Subraman and Murali, J. G. (2021), "Fabrication of A5061 PRMMC by using GTAW process and evaluating the material behaviour", Materials Today, Volume 33, Part 7, 2020, Pages 3169-3173.
[3] Ebrahimzadeh, I., Sadeghi, B., and Maddahi, H., "Welding of thin sheet of Al5456 aluminum alloy by using GTA and GMA welding process", Materials Research Express, Volume 6, Number 6.
[4] Gill, S., and Dhiman, S., "Effect of Intermetallic Compound Deposits on Wear Resistance and Microhardness on AISI 1020 Steel Substrate Using GTAW Process", MATEC Web of Conferences, 221:0100.
[5] Borrisutthekul, R., Seangsai, A., and Paonil, W., "GTAW of Zinc-Coated Steel and Aluminum Alloy", Engineering Journal, Volume 22 Issue 3.
[6] Huang, Y., Wu, V., Lv, N., Chen, H., and Chen, S.," Investigation of porosity in pulsed GTAW of aluminum alloys based on spectral and X-ray image analyses, Journal of Materials Processing Technology, Volume 243, Pages 365-373.
[7] Almenara, M., and Capace, M., "Microstructure and mechanical properties of GTAW welded joints of AA6105 aluminum alloy", Rev. Fac. ing. vol.25 no.43.
[8] Tatsuya SAKIYAMA et.al, Dissimilar Metal Joining Technologies for Steel Sheet and Aluminum Alloy Sheet in Auto Body, NIPPON STEEL TECHNICAL, REPORT No. 103, 91-98 (2013).
[9] A Kostka et.al, On the formation and growth of intermetallic phases during interdiffusion between low-carbon steel and aluminum alloys, Acta Materialia 59, 1586-1500 (2011).
[10] J. Luo et al., Study on the new joining technology of aluminum alloy/Q235 steel dissimilar metal by longitudinal electromagnetic hybrid TIG weldingbrazing method, IEEE, Vol. 11, pp. 1698-1701 (2011).
[11] Mitsuhiro Watanabe et.al., Growth Manner of Intermetallic Compound Layer Produced at Welding Interface of Friction Stir Spot Welded Aluminum/Steel Lap Joint, Materials Transactions, Vol. 52, 5, 953-959 (2011).
[12] John A Taylor et.al., Iron-Containing Intermetallic Phases in Al-Si Based Casting Alloys, Procedia Material Science 1, 19-31 (2012).
[13] Erdemir et al., Formation of Fe-Al intermetallic coating on low carbon steel by novel mechanical alloying technique, Powder technology, Vol. 247, pp. 24-29 (2013).
[14] Gang Zhang et.al, Analysis and modelling of the growth of intermetallic compounds in aluminiumsteel joints, RSC Adv. 7, 37797-37705 (2017).

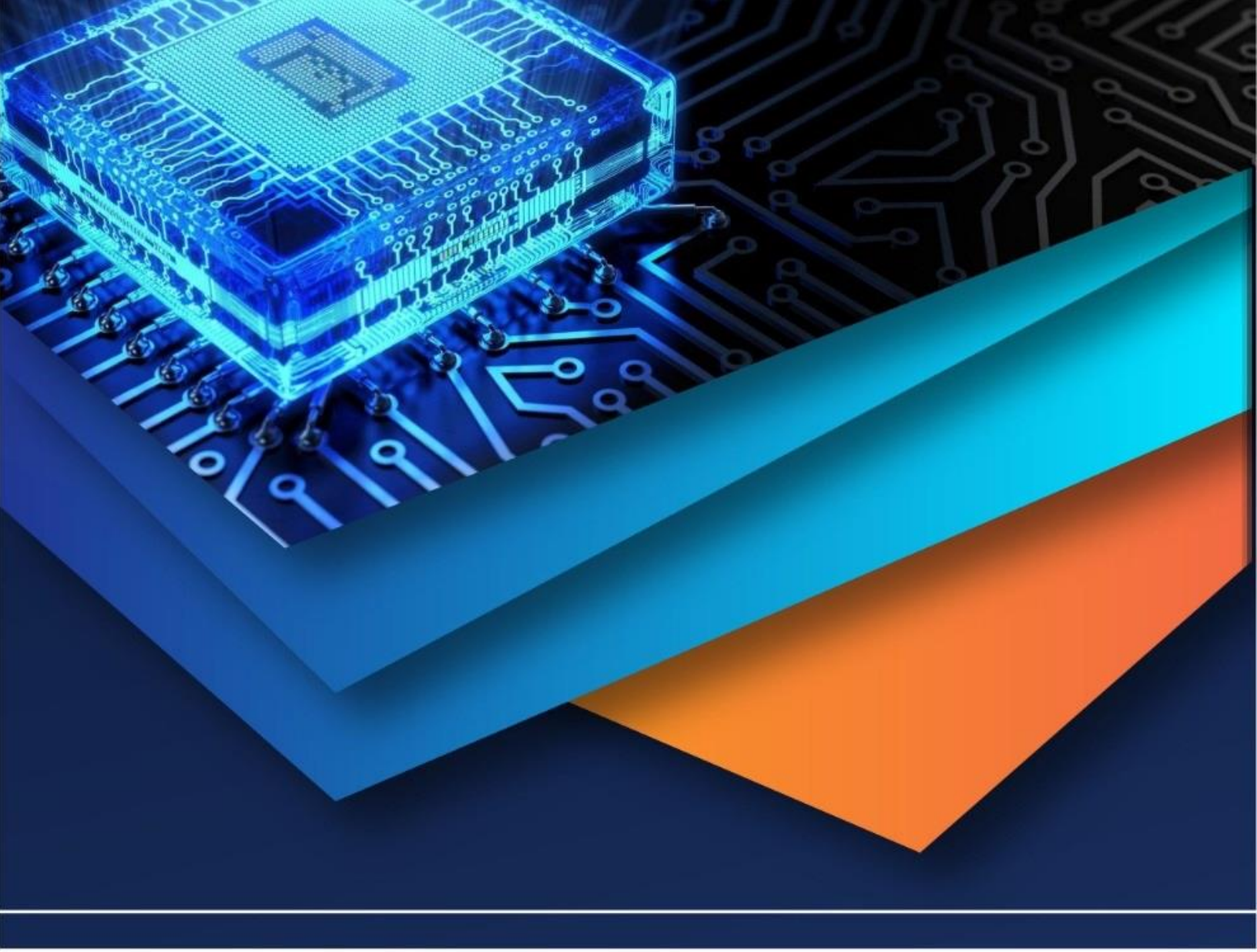

10.22214/IJRASET

45.98

IMPACT FACTOR: 7.129

IMPACT FACTOR: 7.429

INTERNATIONAL JOURNAL FOR RESEARCH

IN APPLIED SCIENCE & ENGINEERING TECHNOLOGY